

# On zonal asymmetry and climate sensitivity

By J. OERLEMANS, *Royal Netherlands Meteorological Institute, Postbus 201, 3730 AE De Bilt, The Netherlands*

(Manuscript received December 5, 1979; in final form March 4, 1980)

## ABSTRACT

The role of zonal asymmetry in climate sensitivity is studied with an annual energy-balance climate model of the Northern Hemisphere. Energy balances are formulated for oceanic and continental regions separately, and coupled through zonal energy transports. Dependent variables are  $\Theta$  and  $T$ , representing sea-level temperature in the oceanic and continental part, respectively. In this model zonal asymmetry is defined as  $\Theta - T$ . It is forced by differences between the oceanic and continental part in (i) the nature of the radiation budget, and (ii) the capacity of transporting energy polewards. The implications of the latter are first illustrated with a simple box model, which can be treated analytically.

The major conclusion of this study is that the sensitivity of the model climate to insolation variations is hardly affected by zonal asymmetry. This result does not depend on the particular set of transport constants used. Temperature drops caused by a 1% decrease in solar constant are in the 1.5 to 2°C range. Experiments are discussed that reveal how the model climate responds to changes in transport constants. It is found that in the 60–70°N latitude belt the present zonal asymmetry ( $\approx 4^\circ\text{C}$ ) is about 1/4 of the value it would have in the absence of zonal energy transport. For the hemispheric mean asymmetry this ratio is about 1/6. Those results indicate that changes in the transport capacities of the ocean-atmosphere system may be of considerable importance with regard to climate sensitivity.

## 1. Introduction

Recently, climate models based on a zonally and vertically integrated energy balance models (acronym EBM in this study) have suggested that the sensitivity of the earth's climate to changes in insolation is rather small. Values of  $\partial T(\varphi)/\partial S$  ( $T$  is annual mean sea level temperature,  $\varphi$  is latitude and  $S$  is normalized solar constant) are typically in the 1.5 to 2.5 K per % range (Oerlemans and Van den Dool, 1978; Coakley, 1979). Such values are far too small to explain pleistocene temperature variations. Evidence exists, nevertheless, that those variations are well correlated with the variability in insolation (Hays et al., 1976). It therefore appears that zonal and annual mean EBM's are not capable of reproducing 'observed' temperature variations.

Some recently made extensions, apart from improving already incorporated parameterizations, are: inclusion of ice sheet-atmosphere feedback (Weertman, 1976; Pollard, 1978; Oerlemans, 1980), incorporating the seasonal cycle (North and Coakley, 1979), accounting for additional albedo

feedback like biosphere adjustment (Cess and Wronka, 1979), and allowing for zonal asymmetry (Hartmann and Short, 1979; North and Coakley, 1979). Hartmann and Short (1979) stressed the potential importance of zonal asymmetry. They used a spectral EBM with linear diffusive energy transport (North, 1975). The zonal asymmetry was introduced by forcing the model with one zonal wave of prescribed amplitude in the radiation budget. With the assumption that the energy diffusivity is equal in zonal and meridional direction, Hartmann and Short computed the zonally asymmetric response in temperature. Although in their model the global forcing of the radiation budget is zero, the response of the global temperature is not because temperature-albedo feedback increase in southward direction due to increasing insolation. This provides the possibility that climatic states with stronger zonal asymmetry and lower temperatures are in equilibrium with the present insolation.

As a next step, this study investigates whether a strong zonally asymmetric forcing can in reality be

maintained. This is done with a model that produces its own asymmetry through differences in planetary albedo over ocean and continent, and through differences in meridional heat transport capacity. The zonal asymmetry created in this way is then reduced by the action of energy transports in zonal direction. The appropriate zonal transport capacity is determined by tuning the model to the present-day zonal asymmetry in the temperature field.

In sections 2 and 3 some observational and simple theoretical considerations on zonal asymmetry in the temperature field are given. The subsequent sections describe the asymmetric EBM and the experiments carried out with it.

## 2. Observational evidence of zonal asymmetry

Fig. 1 shows the sea-land annual temperature difference computed from data processed by Oort and Rosenstien at GFDL (private communication). Those data cover the period 1968–1973. Temperature has been reduced to the 1000 mb level.

Oceanic temperatures are significantly higher than continental temperatures between 45 and 70° N, with a sharp peak at 67° N (the warm

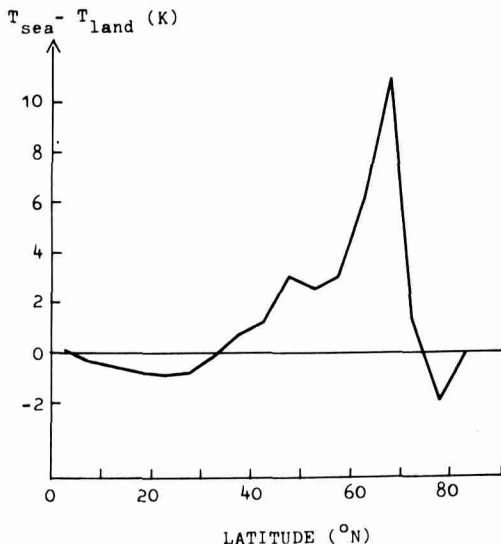


Fig. 1. Difference in sea-level temperature between oceanic and continental regions. The peak at 67° N reflects the warm tongue of the Atlantic Ocean penetrating into high latitudes.

tongue of the Atlantic Ocean). In the subtropics oceanic temperatures are slightly lower. It should be mentioned that the high values mainly result from the conditions in winter, so interaction between zonal asymmetry and the seasonal cycle could be important with regard to climate sensitivity. The studies of Thompson and Schneider (1979) and North and Coakley (1979) indicate that this is not the case, however.

The main causes for the presence of zonal asymmetry are differences in the nature of the radiation budget, and differences in the capacity of transporting energy in meridional direction. Both effects will be incorporated in the model to be used. In order to get an idea of the difference in transport capacity between oceanic and continental regions, we employ observational data from Oort and VonderHaar (1976). We define diffusivities  $D_o$  and  $D_a$  for ocean and atmosphere by

$$F_o = D_o(\partial T/\partial\phi)_o(1 - \Delta) \tag{1a}$$

$$F_a = D_a(\partial T/\partial\phi) \tag{1b}$$

Here  $(\partial T/\partial\phi)_o$  is the meridional temperature gradient in the oceanic part,  $F_o$  and  $F_a$  denote northward energy transports and  $\Delta$  the fraction of land along a latitude circle. We now assume that  $D_a$  is equal over ocean and continent. It is difficult to justify this assumption, in particular since regions of strong poleward energy fluxes are situated over the eastern coasts of the continents. We keep in mind that  $D_a$  might be slightly larger over oceans, thus enhancing the effect of the energy transport by ocean currents. The ratio of the diffusivity in continental regions to that in oceanic regions can be expressed as

$$R = \frac{D_a}{D_a + D_o} = \left[ 1 + \frac{F_o}{F_a} \cdot \frac{(\partial T/\partial\phi)_o}{(\partial T/\partial\phi)_o} \cdot \frac{1}{1 - \Delta} \right]^{-1} \tag{2}$$

Inserting values of  $F_o$  and  $F_a$  from Oort and VonderHaar (1976) and temperature gradients from Oort and Rosenstien leads to Fig. 2. The low values of  $R$  in the subtropics reflect the important role of the oceans in transporting energy towards middle latitudes. North of 60° N, the diffusivity in oceanic regions is smaller than that in continental regions. This is due to weak southward energy transport in the ocean at high latitudes.

In the region of strong poleward energy fluxes, from 20 to 60° N, more energy is transported in the oceanic part than in the continental part. We may

therefore expect that the part of  $(T_{sea} - T_{land})$  induced by this effect is negative at low and positive at high latitudes.

Apart from radiation effects, the zonal asymmetry depends on both meridional and zonal energy transports. To illustrate how this happens, we first consider a simple box model.

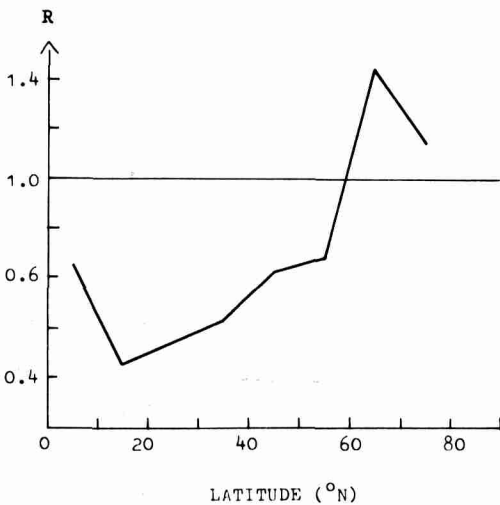


Fig. 2. Ratio of energy diffusivity in continental part to that in oceanic part.

### 3. A simple box model

#### 3.1. Formulation

We divide the earth-atmosphere system in four boxes of equal area: polar oceanic, polar continental, equatorial oceanic and equatorial continental (see Fig. 3). With the assumption that energy fluxes are proportional to surface temperature differences, the energy balances of the boxes may be expressed as

$$Q_{eq} = K(T_{eq} - \Theta_{eq}) + K_c \delta T + a + bT_{eq}, \quad (3)$$

$$Q_{po} = K(T_{po} - \Theta_{po}) - K_c \delta T + a + bT_{po}, \quad (4)$$

$$Q_{eq} = -K(T_{eq} - \Theta_{eq}) + K_o \delta \Theta + a + b\Theta_{eq}, \quad (5)$$

$$Q_{po} = -K(T_{po} - \Theta_{po}) - K_o \delta \Theta + a + b\Theta_{po}. \quad (6)$$

In eqs. (3)–(6),  $Q$  is the net incoming shortwave radiation and  $a + bT$  resp.  $a + b\Theta$  denote the outgoing longwave radiation.  $T$  and  $\Theta$  refer to continental and oceanic temperature, respectively.

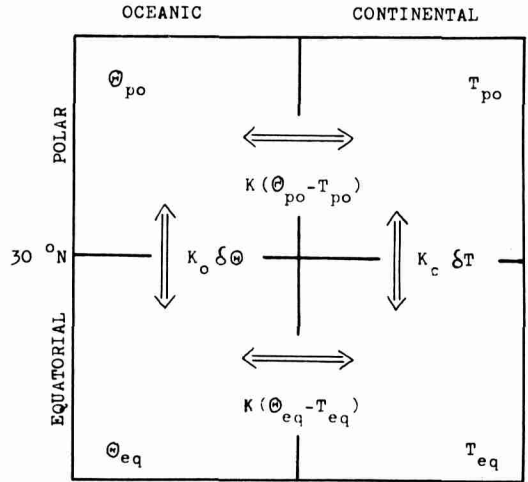


Fig. 3. Schematic picture of a simple model used to illustrate the role of energy transports in creating zonal asymmetry.

$K_c$  and  $K_o$  are meridional transport coefficients in the continental and oceanic part, and  $K$  is the zonal transport coefficient. Further, for any quantity  $\chi$ ,  $\delta\chi = \chi_{eq} - \chi_{po}$ .

In order to isolate the effect of different meridional transport coefficients,  $Q$  is taken equal for oceanic and continental regions. Also,  $Q$  is independent of temperature, so temperature-albedo feedback is not included. A few simple algebraic manipulations lead to the following relations between meridional temperature gradients and transport coefficients:

$$(2K + 2K_c + b)\delta T - (2K + 2K_o + b)\delta \Theta = 0, \quad (7)$$

$$(2K_c + b)\delta T + (2K_o + b)\delta \Theta = 2\delta Q. \quad (8)$$

Eqs. (7) and (8) may be used in several ways. We will do the following exercises with this set. First, we solve for the transport coefficients by inserting observed values of  $\delta Q$ ,  $\delta \Theta$ ,  $\delta T$  and  $b$ . Second, we try to reveal the effect of changes in the zonal transport coefficient  $K$  on  $\delta T$  and  $\delta \Theta$  by keeping  $K_o$  and  $K_c$  equal to the tuned values obtained in the first exercise.

#### 3.2. Solving for the transport coefficients

From the data presented by Ellis and VonderHaar (1976) we find for annual mean conditions  $\delta Q = 159 \text{ W/m}^2$  and  $b = 2 \text{ W/(m}^2 \text{ K)}$ . Values of  $\delta \Theta$  and  $\delta T$  were computed from the data men-

tioned in section 2; they are  $\delta\Theta = 19.6^\circ\text{C}$  and  $\delta T = 21.2^\circ\text{C}$ , so  $\delta T - \delta\Theta = 1.6^\circ\text{C}$ . This rather small value only weakly reflects the difference between continental and oceanic temperatures at middle latitudes. This is due to the poor resolution of the box model. Since this model merely serves as an illustration, this point is not very serious.

Inserting the observed values of  $b$ ,  $\delta Q$ ,  $\delta\Theta$ , and  $\delta T$  in eqs. (7) and (8) leaves two equations with three unknowns:  $K$ ,  $K_o$  and  $K_c$ . In order to solve the set we need an additional relation. One approach is to prescribe  $R^* = K_c/K_o$  (this quantity corresponds to  $R$  in the preceding section). If we now solve eqs. (7) and (8) for various values of  $R^*$ , Fig. 4 results. It shows, for given  $R^*$ , how strong the zonal transport coefficient should be in order to meet present-day conditions. From the figure we see that if  $R^* > 0.9$ , a negative value of  $K$  (resulting in a counter-gradient flux) is required to give the observed temperature difference between oceanic and continental regions. On the other hand, if  $R^* < 0.9$ ,  $K$  should be positive in order to smooth out the temperature differences caused by the larger meridional transport in oceanic regions.

3.3. Changing the zonal transport coefficient

At middle latitudes a typical value of  $R$  is 0.6 (see Fig. 2). Results in the preceding subsection then give  $K_o = 3.65$ ,  $K_c = 2.19$  and  $K = 14.46$

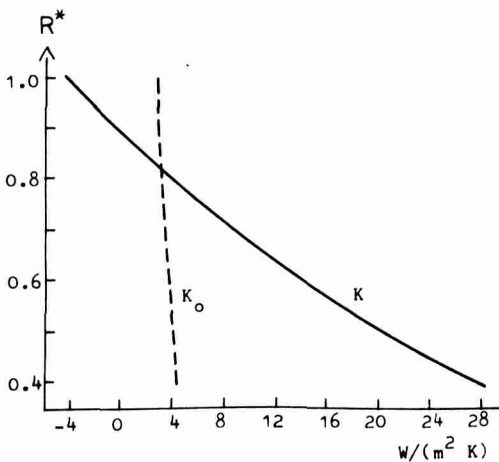


Fig. 4. Relation between transport coefficients resulting from matching the simple box model to present-day conditions.

$W/(m^2 K)$  to match present-day climate. Varying  $K$  and keeping  $K_o$  and  $K_c$  fixed leads to Fig. 5. It shows how the oceanic and continental meridional temperature gradients depend on  $K$ . For  $K \rightarrow \infty$  we have  $\delta T = \delta\Theta = 20.4^\circ\text{C}$ , of course. It appears that  $\delta T$  and  $\delta\Theta$  do not depend strongly on  $K$ : a 50% reduction in  $K$  would lead to a 3% increase in  $\delta T$ .

The sensitivity of temperature gradients on energy diffusivities demonstrates one aspect of zonal asymmetry. It would not be wise to rely on the numerical values given above, but this section may help to understand the results of the less transparent EBM.

4. A zonally asymmetric EBM

4.1. Energy balances over the oceanic and continental parts

The climate model used in this study is an extension of that described in Oerlemans and Van den Dool (1978). The model is based on the energy balances for the oceanic and continental parts of the climate system, i.e.,

$$\begin{aligned} \text{div}(D_o \text{ grad } \Theta) + Q(1 - \alpha_o) &= A_o + B\Theta + CN_o, (9) \\ \text{div}(D_c \text{ grad } T) + Q(1 - \alpha_c) &= A_c + BT + CN_c. (10) \end{aligned}$$

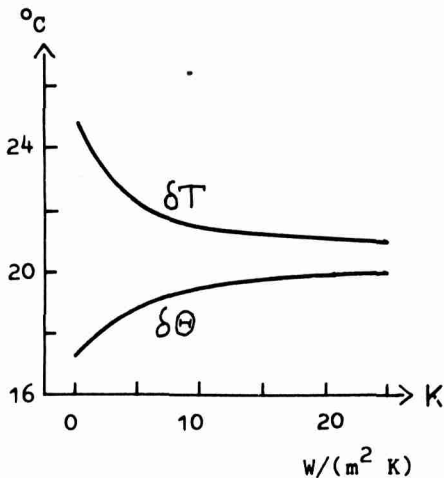


Fig. 5. Relationship between meridional temperature gradients and the zonal transport coefficient  $K$ .  $R^*$  has been set at 0.6.

Here,  $\alpha$  is planetary albedo;  $A$  the constant part,  $B$  the temperature-dependent part, and  $C$  the cloud-dependent part of the outgoing longwave radiation. It was decided to use the same value of  $B$  for the oceanic and continental part, simply because no accurate data were available to make a distinction. The constant  $A$  is allowed to differ, because this provides a straightforward method of tuning the model to the present value of  $\bar{T} - \bar{\Theta}$  (a bar denotes a hemispheric mean value). The fluxes of energy (first terms in eqs. (9) and (10)) are set proportional to the temperature gradients. In the basic formulation of the model,  $D_o$  and  $D_c$  are allowed to vary with latitude and temperature, but are kept constant at first. The constants  $A$ ,  $B$  and  $C$  were taken from Van den Dool (1980). They are based on a regression analysis of radiation-budget data from Ellis and VonderHaar (1976), temperature data from Oort and Rosenstein, and cloud-cover data from Berliand and Strokina (1975). The optimal choice of  $A$ ,  $B$  and  $C$  accounts for 95% of the variance in the outgoing longwave radiation. The values are given in Table 1. Now  $A$  refers to the zonal mean radiation budget.

We now turn to the parameterization of the planetary albedo. We write

$$\alpha = \alpha_s(1 - N) + \alpha_c N$$

where  $\alpha_s$  is clear-sky albedo,  $\alpha_c$  is cloud albedo and  $N$  is cloudiness. The dependence of cloud albedo on the sun's zenith angle is taken into account, because it has a significant influence on the sensitivity of the model climate (Lian and Cess, 1977; Van den Dool, 1980). The clear-sky albedo is expressed in terms of the conditions prevailing at the surface. Snow cover is parameterized by (Oerlemans and Van den Dool, 1978)

$$\text{snow cover} = \begin{cases} 1 & \\ 1 - 0.00033(T_s + 40)^2 & \text{if } T_s < -40^\circ\text{C} \\ 0 & \text{if } -40 \leq T_s < 15^\circ\text{C} \\ & \text{if } T_s \geq 15^\circ\text{C} \end{cases} \quad (12)$$

In eq. (12),  $T_s$  denotes annual mean surface temperature. Sea ice cover is 1 if  $\Theta < -10^\circ\text{C}$  and decreases smoothly to 0 at  $\Theta = 0^\circ\text{C}$ . Snow cover over sea is allowed when sea ice is present. Ice cover on land is represented by ice sheets with simple mechanics. It is assumed that the mass balance of the sheet is a linear function of  $\varphi$  (latitude). In that case the equilibrium size of the Northern Hemisphere ice sheets (measured southwards from  $\varphi = 70^\circ\text{N}$ ) is independent of the absolute mass balance. The position of the southern edge is given by (Oerlemans, 1980)

$$\varphi_{\text{edge}} = \frac{4}{3}\varphi(T^*) - 23^\circ\text{N}, \quad (13)$$

where  $\varphi(T^*)$  is the latitude of the equilibrium point (zero mass balance). This point is coupled to the climate model by attaching it to a sea-level isotherm (denoted by  $T^*$ ). Eq. (13) merely states that the ice-sheet size is 4/3 times the polar sea-equilibrium point distance. In this study the height of the ice sheet was not taken into account.

With the parameterization of the surface conditions just described, and the cloud climatology of Berliand and Strokina (1975), the computation of  $\alpha_s(\Theta)$  and  $\alpha_c(T)$  is easily performed. Values of the constants used are listed in Table 1. The computed albedo for present temperatures is very close to the observed albedo. Relative errors are within 6%, i.e.  $|\alpha_{\text{cal}} - \alpha_{\text{obs}}|/\alpha_{\text{obs}} < 0.06$ .

#### 4.2. Including zonal transport

To prevent meridional transports from contributing to the transport from oceanic to continental regions, the fraction of land is set constant ( $\Delta = 0.4$ ). This corresponds best to the situation in the Northern Hemisphere. The height of the land is set equal to 300 m everywhere, implying that over land surface temperatures (to be used in the radiation computations) are  $2^\circ\text{C}$  lower than the corresponding sea-level temperatures.

Zonal energy transport, from the oceanic to the continental part of the model, may be included by adding the terms  $D(\Theta - T)/(\Delta - 1)$  and  $D(\Theta - T)/\Delta$  to the energy balances (9) and (10), respec-

Table 1. Constants used in the parameterization of the energy balance. The clear sky albedo is divided into four classes as indicated

$A$	233 W/m <sup>2</sup>
$B$	2.04 W/(m <sup>2</sup> k)
$C$	-28.8 W/m <sup>2</sup>
$\alpha_s$ snow cover	0.61
$\alpha_s$ ice cover	0.56
$\alpha_s$ land	0.22
$\alpha_s$ sea	0.13
$T^*$	-8°C

tively. In principle  $D$  is a function of latitude, but we will start our series of experiments with  $D = \text{constant}$ .

#### 4.3. Method of solution

To find equilibrium solutions, the following procedure was carried out. First, starting with some initial temperature field, eqs. (9) and (10) are solved by the iterative method described in Oerlemans and Van den Dool (1978). Zonal transports of energy are then easily computed from  $\Theta(\varphi)$  and  $T(\varphi)$ , and the energy balances are solved again with the energy sources/sinks resulting from the zonal transports to give new estimates of  $\Theta$  and  $T$ . This procedure is repeated until a stable equilibrium solution is reached. Convergence appeared to be most rapid when the temperature series were damped by replacing  $\Theta_{i+1}$  and  $T_{i+1}$  by  $a\Theta_{i+1} + b\Theta_i$  and  $aT_{i+1} + bT_i$ , where  $a + b = 1$ . The optimal values of  $a$  and  $b$  depend on  $D$ ,  $D_c$  and  $D_o$ . For all experiments described here,  $a = 0.3$  and  $b = 0.7$  gave satisfactory convergence. It should be noted that this method gives only internally stable equilibrium solutions; unstable solutions will never be found.

### 5. Varying $D$ , $D_c$ and $D_o$

A large set of experiments was carried out to see which set of transport coefficients simulates the present climate best. In each experiment,  $R (=D_c/D_o)$  was fixed a priori.  $A_o$  and  $A_c$  were then adjusted to give the observed  $\bar{\Theta}$  and  $\bar{T}$ . Meridional and zonal temperature gradients were optimized by searching the best values of  $D_o$  and  $D$ . This procedure was repeated until the best simulation appeared to be reached. Since  $\bar{\Theta}$  and  $\bar{T}$  depend only slightly on the energy transports, a few iterations were sufficient.

Fig. 6 shows how  $D$ ,  $D_o$  and  $D_c$  are related in the case of best fit to present-day conditions, once  $R$  is fixed. The 'quality' of the climate simulation, measured by  $\gamma = \text{RMS}(\Theta, \Theta_{\text{obs}}) + \text{RMS}(T, T_{\text{obs}})$ , where RMS denotes root-mean-square difference with regard to latitude, is almost constant for  $R$  between 0.4 and 0.6 (see Table 2). Comparing Fig. 6 to the corresponding figure of the box model (Fig. 4), we see that  $D$  is much smaller than  $K$ . This is due to the underestimation of  $\Theta - T$  in the simple box model. Qualitatively, however, the picture is the same.

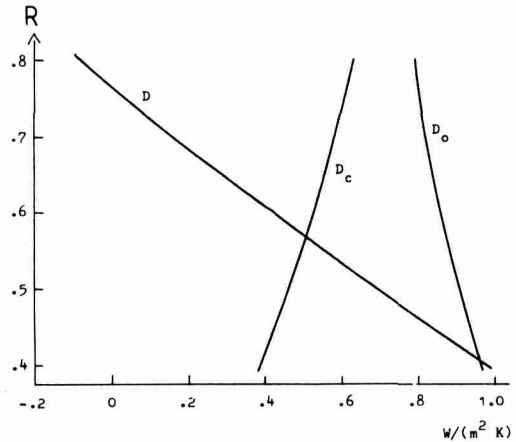


Fig. 6. Relation between transport coefficients, found by requiring that the zonally asymmetric EBM simulates the present distribution of oceanic and continental temperature.

Table 2 lists some output of the experiments. All model versions used to derive Fig. 6 were run with a 1% decrease in solar constant  $S$ . Temperature drops associated with this decrease in  $S$  are shown. Apparently, the sensitivity of the model climate is practically independent of the particular set of transport constants used. The results also showed that  $\partial T/\partial S$  depends only weakly on latitude. The sensitivity in the continental mid- and high latitudes is not enhanced by introducing zonal asymmetry. Moreover, it appears to be the less sensitive region of the model climate, though differences are very small.

### 6. Experiments with more realistic energy transports

#### 6.1. Modification of the energy-transport parameterization

Since in the Northern Hemisphere the mid-ocean to mid-continent distance decreases with latitude, it is not very realistic to use a latitude-independent zonal transport coefficient. A more appropriate way to include zonal energy transport may be the following. A characteristic windspeed for mixing of oceanic with continental air may be defined as  $V^*(\varphi) = \bar{u}(\varphi) + \sigma_u(\varphi)$ , where  $u$  is the zonally-averaged zonal windspeed, the tilde denotes a time mean value, and  $\sigma_u$  is the standard deviation of  $u$

Table 2. Summary of results of the various model versions (obtained by matching present-day conditions once  $R$  is fixed). The last four columns give temperature drops resulting from a 1% decrease in the solar constant

$R$	$\gamma$ (°C)	$A_o$ (W/m <sup>2</sup> )	$A_c$ (W/m <sup>2</sup> )	$\Delta\bar{\Theta}$ (°C)	$\Delta T$ (°C)	$\Delta T_{62}$ (°C)	$\Delta(\bar{\Theta} - T)_{62}$ (°C)
0.4	3.222	228.8	228.0	-1.49	-1.52	-1.48	-0.08
0.5	3.216	229.3	227.4	-1.50	-1.55	-1.52	-0.09
0.6	3.216	231.0	225.0	-1.54	-1.61	-1.55	-0.13
0.7	3.298	231.8	223.7	-1.51	-1.61	-1.50	-0.10
0.8	3.276	232.2	222.8	-1.42	-1.64	-1.50	-0.05

with respect to time. Windspeed is taken at the 850 mb level. The ocean-continent distance varies with  $\cos \phi$ . We may thus introduce a latitude-dependent effective mixing length for zonal energy transport by replacing  $D$  by  $CV^*(\phi)/\cos \phi$ . Here,  $C$  is some constant to be found by tuning the model to the observed zonal asymmetry.

Another modification involves the meridional heat transport by ocean currents. It has frequently been mentioned that vanishing energy transports in the ocean due to sea-ice cover increases the sensitivity of the high-latitude climate. Present-day conditions indicate that oceanic heat transport is small or even equatorward at high latitudes (Fig. 2), but it is unlikely that this may be fully attributed to sea-ice cover.

Anyway, the upward heat flux through ice is much smaller than through a water surface (e.g. Maykut, 1978), so the contribution of the ocean to heating the air must be considerably smaller. We incorporate this effect by the condition

$$D_o = D_c \quad \text{if} \quad \Theta < -5^\circ\text{C}, \quad (14)$$

so oceanic heat transport vanishes if the ice cover is more than 50%. This representation is very crude, but it serves our purpose.

6.2. Simulation of the present climate

Fig. 7 shows how the model, including the modifications of the energy transport, simulates the present zonal mean temperature distribution. Again,  $D_c/D_o = 0.6$ . Also shown are observed values (+) and results of a model run with both  $D_o$  and  $D$  independent of latitude. A similar comparison for the zonal asymmetry is given in Fig. 8.

The results of the modified model are substantially better on two points. First, polar tem-

peratures are closer to observations, which is a result of the decreased meridional diffusivity in the

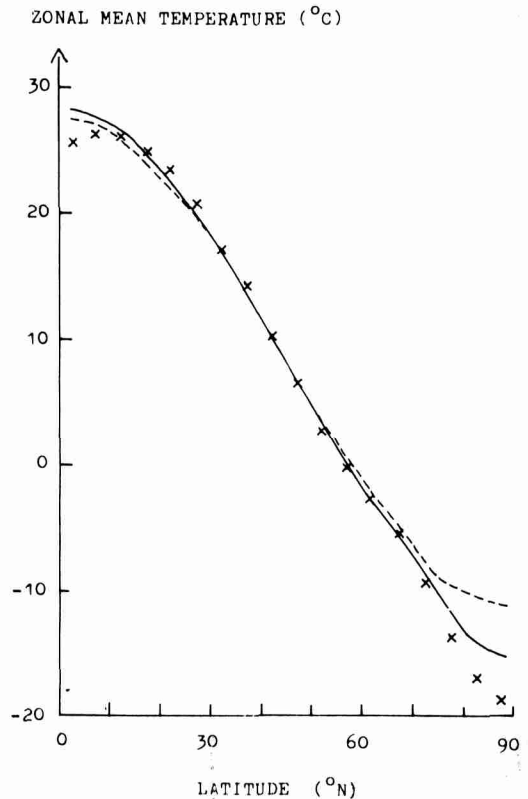


Fig. 7. Model simulation of annual sea-level temperature in the Northern Hemisphere. Dashed line: all transport coefficients independent of latitude and temperature. Solid line:  $D_o$  equals  $D_c$  if  $\Theta$  drops below  $-5^\circ\text{C}$ , and  $D$  depends on latitude. Crosses indicate observed values.

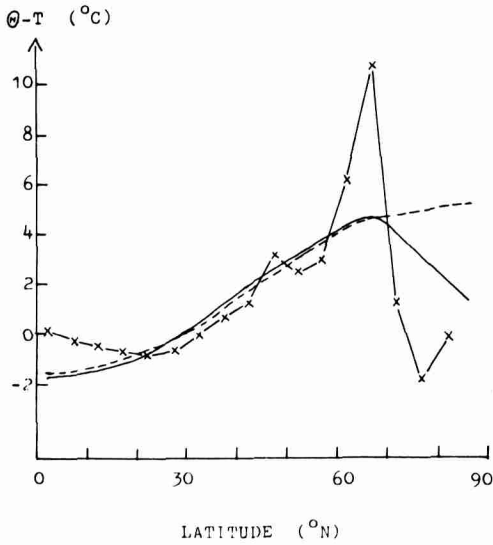


Fig. 8. Same as Fig. 7, but now for the temperature difference between oceanic and continental regions.

oceanic part. Second, the zonal asymmetry in temperature appearing in the modified model shows a more realistic distribution at high latitudes. The lower values of  $\Theta - T$  north of  $70^\circ N$  are the result of the large "effective mixing length" in that region. Altogether, the model provides a satisfactory simulation of the present temperature distribution. In our further experiments, we will use this model version.

**7. Variation of insolation**

In this section we study the sensitivity of the model climate to changes in insolation.

Fig. 9 shows the temperature drop resulting from a 2% decrease in  $S$  (solar constant). The temperature drop at high latitudes is larger than at low and middle latitudes; maximum sensitivity occurs at  $\varphi = 72^\circ N$ . This peak is essentially due to the albedo feedback (see Van den Dool, 1980 for a discussion on this point), while the higher sensitivity for the whole region north of  $65^\circ N$  comes from the reduction of heat transport by the ocean (eq. (14)). At low and middle latitudes the picture is different. In particular, around  $35^\circ N$  the temperature drop over land is much larger than that over sea. This may be attributed to the fact that, for

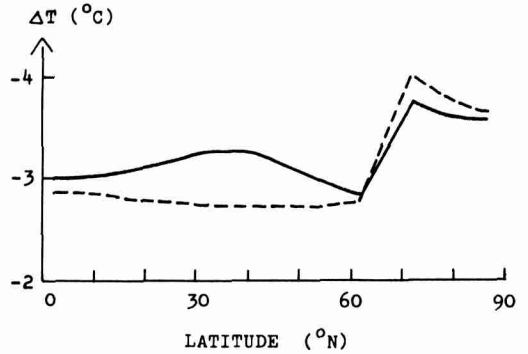


Fig. 9. Temperature drop resulting from a 2% decrease in solar constant. Dashed and solid line apply to oceanic and continental temperature, respectively.

temperatures in the  $0$  to  $15^\circ C$  range, temperature-albedo feedback occurs only in continental regions. Moreover, at middle latitudes cloudiness is substantially lower (about 20%) over land, which makes the temperature-albedo feedback more effective. A model run with minimum obliquity of the earth gave temperature changes (with respect to present conditions) gradually changing from  $-0.6^\circ C$  at the pole to  $+0.3^\circ C$  at the equator, with very little difference between oceanic and continental regions. The experiments just described were also carried out with a model not including zonal asymmetry, but with essentially the same parameterizations. The experiments showed that the sensitivity of the model climate is hardly affected by the incorporation of zonal asymmetry. Changes in the characteristic temperature drops shown in Fig. 9 are not more than  $\pm 20\%$ .

**8. The potential of varying transport constants**

It has sometimes been argued that during glacial epochs strong planetary waves substantially change the pattern of advection of energy, which may cause large changes in the energy balances over sea and ocean. Variation of energy diffusivities in our climate model can give a crude estimate of the potential importance of such processes. This importance is ultimately determined by differences in the nature of the radiation budget. For example, if the radiation budgets over ocean and continent vary with insolation in the same way, differences in zonal transport do not affect the sensitivity.

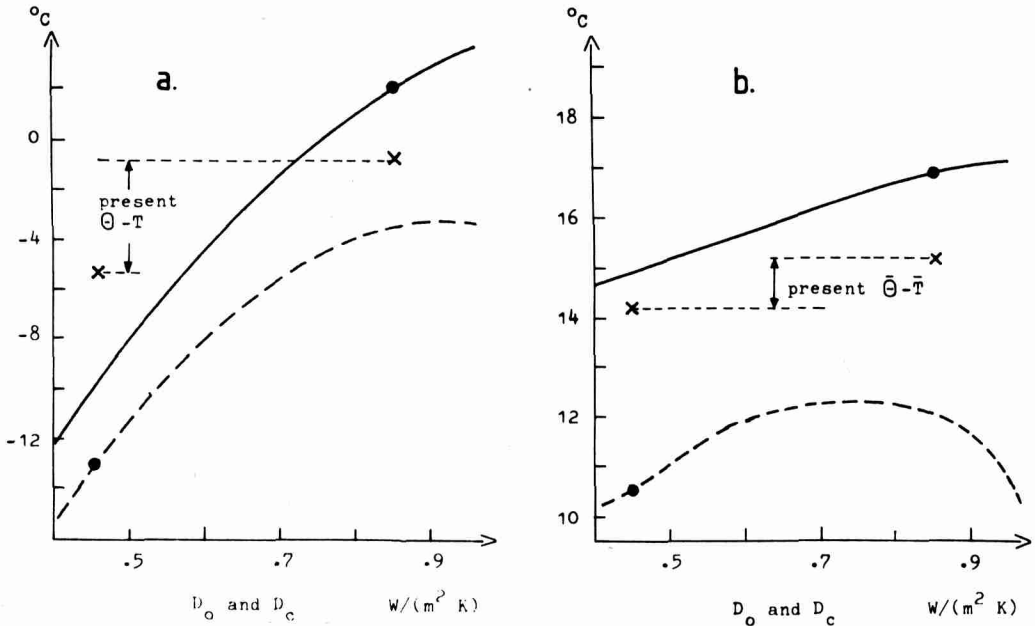


Fig. 10. Continental (dashed) and oceanic (solid) temperature at  $62^\circ\text{N}$  (a) and averaged over the Northern Hemisphere (b), as a function of the meridional transport coefficient. The oceanic and continental energy balances have been decoupled ( $D = 0$ ). Crosses indicate present-day temperatures, black spots temperatures that would exist if  $D = 0$  with the same meridional transport coefficients as today.

We look at what happens if zonal transports vanish completely. Fig. 10 shows some results of runs with  $D = 0$ . In this case the energy balances over sea and land are independent. Since meridional transports may also change, a range of values of  $D_o$  and  $D_c$  was investigated.

Fig. 10a shows  $\Theta$  and  $T$  at  $62^\circ\text{N}$  latitude. Present temperatures (=best model simulation) are indicated by crosses. Black spots give values that would appear if  $D$  is set to zero without changing the meridional energy diffusivities. In this case  $\Theta_{62} - T_{62}$  would be almost 4 times as large as at present, which illustrates the important role of zonal energy transport in maintaining the present climate. From the figure we see that at high latitudes zonal asymmetry is enhanced by a lower value of  $D$  and a higher value of  $D_o - D_c$ .

Fig. 10b shows the same, but now for hemispheric mean temperatures. At present, the hemispheric zonal asymmetry is only 1/6 of its potential value. It is interesting that for high values of  $D_c$  low values of  $\bar{T}$  occur. Here the albedo-temperature

feedback is allowed to penetrate to lower latitudes. The results displayed in Fig. 10 cannot provide more than a crude estimate of how the climate system responds if energy transports change. The differences in the radiation budget over land and ocean appearing in the climate model depend on tuned values of  $A_o$  and  $A_c$ , and to the cloud climatology used. Since those quantities are not accurately known, results should not be taken too literally.

## 9. Discussion

The most important conclusion to be drawn from this study is that the incorporation of zonal asymmetry in an annual mean EBM hardly effects the sensitivity of the model climate with regard to changes in insolation. This result does not depend on the particular set of transport constants used (see Table 2). Only if insolation variations would induce large changes in the transport capacities of the climate system, temperature responses could be

comparable in magnitude to "observed" pleistocene temperature variations.

To assess the value of this conclusion, we have to reconsider the internal freedom of the model. The crucial question is to what extent the present model is capable of producing differences in zonal asymmetry for different forcing. Factors that may force changes in zonal asymmetry are:

- different albedo feedback over continent and oceanic regions,
- different IR feedback (cloudiness over sea differs from that over land),
- cut-off of energy transport by the oceans if sea ice is present.

Differences in meridional energy transport can interfere in various ways with those components, while zonal energy transport always tends to destroy changes in zonal asymmetry. Although in the present model cloudiness over sea and land and the transport capacities are fixed, it appears that

the model has some internal freedom to create changes in zonal asymmetry. But why does this not happen?

In the model, the largest forcing of zonal asymmetry occurs between the sea-ice boundary and the boundary of the 25% snow/ice cover over land. For smaller values of  $S$  this zone should shift southward, thus increasing the value of  $\Theta - T$  at middle latitudes and decreasing it at higher latitudes. The meridional energy transports, however, smooth out the temperature field so strongly that this effect is almost completely lost. In addition, the zonal and meridional heat transports act in a complementary way: they try to conserve both the meridional and zonal temperature gradients. The combination of small differences in albedo feedback over land and ocean and the very effective redistribution of energy make the zonal asymmetry of the model climate so insensitive to changes in insolation, and so sensitive to changes in the transport capacities.

#### REFERENCES

- Berliand, T. G. and Strokina, L. A. 1975. Cloud regime over the globe. *Proceedings of GGO, Physical Climatology*, No. 338, Leningrad.
- Cess, R. D. and Wronka, J. C. 1979. Ice ages and Milankovitch theory: A study of interactive climate feedback mechanisms. *Tellus* 31, 185–192.
- Coakley, J. A. 1979. A study of climate sensitivity using a simple energy balance model. *J. Atmos. Sci.* 36, 260–269.
- Ellis, J. S. and VonderHaar, T. H. 1976. *Zonal average earth radiation budget measurements from satellites for climate studies*. *Atm. Sci. Paper No. 240*, Colorado State University.
- Hartmann, D. L. and Short, D. A. 1979. On the role of zonal asymmetries in climate change. *J. Atmos. Sci.* 36, 519–528.
- Hays, J. D., Imbrie, J. and Shackleton, N. J. 1976. Variations in the earth's orbit: pacemakers of the ice ages. *Science* 194, 1121–1132.
- Lian, M. S. and Cess, R. D. 1977. Energy balance climate models: a reappraisal of ice-albedo feedback. *J. Atmos. Sci.* 34, 1058–1062.
- Maykut, G. A. 1978. Energy exchange over young sea ice in the central Arctic. *J. Geophys. Res.* 83, 3646–3658.
- North, G. R. 1975. Theory of energy-balance climate models. *J. Atmos. Sci.* 32, 2033–2043.
- North, G. R. and Coakley, J. A. 1979. Differences between seasonal and mean annual energy balance model calculations of climate and climate sensitivity. *J. Atmos. Sci.* 36, 1189–1204.
- Oerlemans, J. 1980. On continental ice sheets and the planetary radiation budget. Submitted to *Quaternary Research*, in press.
- Oerlemans, J. and Van den Dool, H. M. 1978. Energy balance climate models: stability experiments with a refined albedo and updated coefficients for infrared emission. *J. Atmos. Sci.* 35, 371–381.
- Oort, A. H. and VonderHaar, T. H. 1976. On the observed annual cycle in the ocean-atmosphere heat balance over the Northern Hemisphere. *J. Phys. Oceanogr.* 6, 781–800.
- Pollard, D. 1978. An investigation of the astronomical theory of the ice ages using a simple climate-ice sheet model. *Nature* 272, 233–235.
- Thompson, S. L. and Schneider, S. H. 1979. A seasonal zonal energy balance climate model with an interactive lower layer. *J. Geophys. Res.* 84, 2401–2414.
- Van de Dool, H. M. 1980. On the role of clouds in an energy balance climate model. *J. Atmos. Sci.* 37, in press.
- Weertman, J. 1976. Milankovitch solar radiation variations and ice age ice sheet sizes. *Nature* 261, 17–20.

## О ЗОНАЛЬНОЙ АСИММЕТРИИ И ЧУВСТВИТЕЛЬНОСТИ КЛИМАТА

С помощью среднегодовой энергобалансовой климатической модели Северного полушария исследуется роль зональной асимметрии чувствительности климата. Балансы энергии формулируются отдельно для океанических и континентальных областей и связываются через зональные переносы энергии. Зависимыми переменными являются  $\theta$  и  $T$ , представляющие температуру на уровне моря в океанической и континентальной части, соответственно. В этой модели зональная асимметрия определяется как  $\theta - T$ . Она вынуждается различиями между океанической и континентальной частями в природе (а) радиационного бюджета и (б) в способности переносить энергию к полюсу. Роль последнего сначала иллюстрируется с помощью ячейковой модели, которая может трактоваться аналитически. Основной вывод данного исследо-

вания состоит в том, что зональная асимметрия слабо воздействует на чувствительность модели климата к вариациям инсоляции. Этот результат не зависит от частного набора используемых констант переноса. Понижения температуры, вызванные уменьшением на 1% солнечной постоянной, лежат в пределах от 1,5 до 2°C.

Обсуждаются эксперименты, которые обнаруживают, как модельный климат отвечает на изменения в константах переноса. Найдено, что в широтном поясе 60–70° с.ш. современная зональная асимметрия ( $\approx 4^\circ\text{C}$ ) около 1/4 от величины, которая была бы в отсутствие зонального переноса энергии. Для средней асимметрии полушария это отношение около 1/6. Эти результаты указывают, что изменения в способности переноса системы океан-атмосфера могут быть существенны для чувствительности климата.